Using Argo data to investigate the Meridional Overturning Circulation in the North Atlantic

Alonso Hernández-Guerra[a], Terrence M. Joyce[b], Eugenio Fraile-Nuez[c], and Pedro Vélez-Belchí[c]

[a] *Facultad de Ciencias del Mar, Universidad de Las Palmas de Gran Canaria, 35017 Las Palmas, Spain (e-mail: ahernandez@dfis.ulpgc.es).*

[b] *Department of Physical Oceanography, Woods Hole Oceanographic Institution, 360 Woods Hole Rd., Mail Stop 21, Woods Hole, Mas. 02543, USA (e-mail: tjoyce@whoi.edu; tel: 508-289-2530; fax: 508-457-2181).*

[c] *Instituto Español de Oceanografía, Avenida Tres de Mayo, 73, 38005 Santa Cruz de Tenerife, Spain (e-mails: eugenio.fraile@ca.ieo.es; pedro.velez@ca.ieo.es).*

***Corresponding author**: Terrence M. Joyce. Department of Physical Oceanography, Woods Hole Oceanographic Institution, 360 Woods Hole Rd., Mail Stop 21, Woods Hole, Mas. 02543, USA (e-mail: tjoyce@whoi.edu; tel: 508-289-2530; fax: 508-457-2181).*

Abstract

Using a variety of oceanographic data, including direct volume transports in the Florida Strait, and Argo float profiles and drift velocities at 24 and 36N in the North Atlantic, inverse calculations are presented in which the net meridional transport, down to a depth of approximately 1600 m, is estimated at both latitudes for a five year period 2003-2007. The upper ocean is divided into 7 layers using neutral density, and mass conservation constraints have been applied to a closed box bounded by these latitudes, including the Florida Strait. Ekman layer transports have been included in the top-most layer, and the inverse calculation has solved for changes from the initial reference velocities, Ekman and Florida Strait transports, given *a priori* estimates on the accuracy of each of these quantities. Solutions with and without transformations due to Mediterranean Water (MW) formation are made. Our results indicate that 1) time-averaged transport estimates derived from Argo have significant less eddy noise than individual hydrographic sections, 2) Argo drift velocities provide information to the inverse solution for the ocean interior, and 3) comparison of the total integrated interior mass transports in the thermocline waters for the period 2003-2007 with the previous estimates based on trans-ocean hydrographic sections shows that the Meridional Overturning Circulation has not significantly changed since 1957.

Keywords: Meridional Overturning Circulation; Argo floats; objective analysis; box inverse model.

1. Introduction

The global ocean observing system has evolved to the point that the goal is already achieved of having 3000 autonomous floats providing temperature and salinity profiles from the surface to 2000 m at regular (e.g. 10 day) intervals. This Argo system (ArgoScienceTeam, 1998) also provides estimates of velocity at the 'parking depth' of each float (Yoshinari et al., 2006). We are taking advantage of this system to investigate the decadal variation of the Meridional Overturning Circulation (MOC) in the North Atlantic at mid latitudes and thus to check the robustness of a recent result suggesting that a decline of the MOC at mid latitudes as obtained by Bryden *et al.* (2005b) is due to intra-annual variability (Cunningham et al., 2007). This MOC involves the poleward transport of upper ocean waters and an equatorward transport of deeper, colder waters. A decline of the MOC has been one of the predictions of various IPCC reports on greenhouse gas scenarios (IPCC, 2001). A particular aspect of the recent findings from a single hydrographic section at 24N in 2004 is that more equatorward flow is contained in the interior of the upper 1000m than previously observed. The nature of those calculations is that, while deep flows are not directly measured, a combination of top-to-bottom hydrography, estimates of the northward flow in the Florida Strait, and of the wind-forced upper Ekman layer, can all be combined to yield an estimate of net flow throughout the water column, using the constraint that no net meridional flow exists across a complete zonal section. Thus, increasing geostrophic shear and equatorial flow in the upper layers of the ocean interior will translate into less equatorward flow of the deeper waters below the wind-driven layers, since both the Ekman and Florida Current transports are poleward at this latitude. These deeper layers, called collectively North Atlantic Deep Water (NADW) are comprised of Labrador Sea Water and the Lower Deep Water, which is largely derived from overflows from the Greenland, Iceland, Norwegian Seas. A reduction in the MOC refers to the fact that there is less conversion of upper to lower waters at high latitudes, and thus less meridional heat flux in this overturning circulation (Bryden and Imawaki, 2001).

2. Data and methods

All available, good quality Argo data from the five year period 2003-2007 in the North Atlantic (Fig. 1a) have been examined, edited, calibrated for salinity (Wong et al., 2003) and objectively interpolated onto hypothetical zonal 'sections' at 24 and 36N (Fig. 1b), following a method employed previously (Fraile-Nuez and Hernandez-Guerra, 2006). The statistical approach used, optimal statistical interpolation, is commonly used to obtain climatological fields, since it has been designed to minimize the signal to noise ratio, being the noise mainly due to eddies in transoceanic sections (Pedder, 1993). To take into account the different dynamics, as the Sverdrup dynamics and the Gulf Stream return flow, the optimal statistical interpolation scheme is applied to different subregions. The procedure used gives an estimate of temperature and salinity mean fields for the period 2003-2007. The objective analysis also provides an estimation of the error in the temperature and salinity mean field. Fraile-Nuez and Hernandez-Guerra (2006) estimated them from an objective analysis using Argo data in the Eastern North Atlantic Subtropical Gyre. The estimated error was 0.48°C/0.10 in temperature/salinity at the surface layer decreasing to 0.04°C/0.01 at depth deeper than 27.922 γ_n. Hadfield *et al.* (2007) estimated that the RMS difference between Argo profiles interpolated to positions of the hydrographic section carried out at 36N by Bryden *et al.*, (2005b) and the *in situ* hydrographic measurements is 0.6°C, smaller in the eastern basin, less than 0.4°C, and larger in the western boundary, up to 2°C. This high error estimate is probably due to the low sampling by Argo profiles in the western boundary because these authors only chose 2 months of Argo profiles before and after the hydrographic cruise. Contrary, we have chosen five year period and the western boundary is well sampled as shown in Figure 1.

The 5 year span with similar number of profiles for each month substantially reducing effects of monthly variability suggested by (Wunsch and Heimbach, 2006). Figure 2 shows the vertical sections of temperature and salinity for each section divided into 7 layers determined by neutral density (γ_n) (Jackett and McDougall, 1997). Initial geostrophic flow is estimated using a deep zero velocity surface at 27.922 γ_n. Estimates of float drift at 1500 m in the eastern basin and 1000 m in the western basin (Fig. 1c) provide additional constraints on the circulation (Fig. 3). Velocity estimates, using the same procedure as for the hydrographic data, are also objectively estimated at every half degree of longitude at 24 and 36N. For objectively interpolated temperature and salinity, the annual climatological temperature and salinity data from WOA94 (World Ocean Atlas, 1994) is used as a first guess (Levitus and Boyer, 1994; Levitus et al., 1994), while for velocities at the parking depth, instead, the mean velocity for each longitude interval is used. The large amount of data and the 5 year span of observations allow the ocean 'eddy' noise, always present in single hydrographic sections, to be greatly reduced as indicated by the fact that the noise to signal ratio obtained during the objective analysis of the ARGO sections at 24N and 36N is an order of magnitude smaller than that for a single hydrographic section. In particular, the noise to signal ratio is 0.08 for the ARGO 24N temperature section, meanwhile the ratio is 1.27 and 0.68 for the WOCE A05 1992 (Parrilla et al., 1994) and the WOCE AR01 1998 (Baringer and Molinari, 1999) sections, respectively.

3. Results and conclusions

In the mean hydrographic section obtained at 24N (Fig. 2) a relatively smooth deepening of the thermocline (traced by the 11C isotherm) towards the west is observed, with the deepest depths just to the west of 70W. The 36N section shows more variability, with a deep thermocline over a broad longitude range from 45 to 70W, after which it shoals rapidly to the west. We will later see that this region of a deep thermocline at 36N is part of the southern recirculation gyre of the Gulf Stream (Hogg, 1992). The rapid thermocline shoaling and a corresponding freshening to the west of 70W is signature of the separated Gulf Stream just east of Cape Hatteras. The salinity signal at 36N also shows a clear influence of salty Mediterranean Water to the east of the Mid-Atlantic Ridge, which is seen as the shallow spikes in bathymetry between 30 and 35W.

While it is common to use the net transport through Florida Strait as a constraint, the procedure used requires that this transport be prescribed as a function of density layers. We use a section of density and geostrophic velocities relative to a deepest common level from 1998 carried out by Baringer and Molinari (1999) together with an uniform, depth-independent velocity of 22 cm/s to make the total transport 32.4 Sv (Baringer and Larsen, 2001). Throughout this paper the unit Sv will be used to indicate both mass transport (1 Sv=10^9 kg/s) and volume transport (1 Sv=10^6 m^3/s). There is no corresponding accepted transport figure for the western end of 36N, although previous studies carried out by Halkin and Rossby (1985) have shown a much enhanced Gulf Stream transport over and above that in the Florida Strait. We thus rely on the Argo data in this region, but will allow the inverse solution some flexibility because this transport is not well-constrained by the float velocity data. From the study of Halkin and Rossby (1985), the mean and standard deviation of repeated sections across the Gulf Stream at 36N, 73W, showed mean northward currents of 10-20 cm/s at our float velocity reference level of 1000m, with comparable standard deviation. The interior wind-driven flow in the Ekman layer is calculated from the mean wind stress in the period 2003-2007 estimated from QuikScat satellite measurements. The inverse model allows small adjustments to the Ekman transport to satisfy transport constraints.

If one constructs a box with a northern boundary at 36N, a southern boundary at 24N, including the Florida Strait, then one can place constraints on the flow based, for example, on the assumption that there is no net mass transport divergence for any of the seven density layers used. These layers include a surface layer which carries the Ekman transport, four uppermost layers characterizing the waters of the thermocline (layers 1:4), extending down to those containing the upper portions of Labrador Sea Water (Layers 6:7). We show (Table 1) the various portions of the budget for mass transport in the box. Using no *a priori* velocity information, except a zero geostrophic velocity surface at γ_n =27.922, yields a net transport across the southern side of the box of 33.5 Sv and 27.4 Sv out at the northern boundary. Clearly the initial guess velocity field is in need of some adjustment. With the velocity information from the Argo floats and for the Florida Strait, we now obtain 24.0 Sv flow into the box from the south and 11.5 Sv out the box from the north, suggesting further adjustments are still required to fulfil necessary assumption within the box. With the well-established Gauss-Markov Inverse method (Wunsch, 1996), one can obtain revised transports with uncertainty which will satisfy a mass balance overall and in each of the 7 layers, given some estimates of error in the required mass balance, and in the *a priori* velocity information for the 258 station pairs. The preliminary variance assigned to the velocities are $(4\ \mathrm{cm/s})^2$ to the two closest station pairs at the eastern and western boundaries of 24N and eastern boundary of 36N, $(15\ \mathrm{cm/s})^2$ from 70 to 75W at 36N that corresponds to the offshore extension of the Gulf Stream, $(2\ \mathrm{cm/s})^2$ for station pairs over the open ocean, and $(1\ \mathrm{cm/s})^2$ for Florida Strait. The inverse model also allows an adjustment of 20% to the initial Ekman transport. For the *a priori* variance for each equation, we follow the idea that mass transport at surface layers present a higher variance than deeper layers. Thus, we select values of $(2\ \mathrm{Sv})^2$ for the first layer, $(1.5\ \mathrm{Sv})^2$ for the second layer, $(1\ \mathrm{Sv})^2$ for layers 3 and 4, $(0.5\ \mathrm{Sv})^2$ for layers 5 to 7, and $(2\ \mathrm{Sv})^2$ for the overall constraint. Results are, of course, sensitive to these error estimates. A sensitivity test of the solution is presented in the Appendix.

For our choices, we obtain the balances given for the 'Inver. Mod. Veloc.' (Table 1, and Fig. 4). The Ekman and Florida Current transports have changed somewhat, as have the initial reference velocities (Fig. 3). Although we started with a quite large Ekman transport obtained from satellite data, 5.3 Sv at 24N, the adjusted Ekman transport at 24N is not significantly different to that used by Bryden *et al.* (2005b): 3.8 and 3.6 Sv, giving further confidence in the inverse model results. The largest changes being for the 36N velocities west of 70W: the region where representation of the mean Gulf Stream flow is poorly defined by the floats. We have divided the transport figures from Table 1 into two multi-layer estimates: one for the thermocline waters (layers 1:4), and one for the remainder three layers (5 to7).

In this table, we also show the 'Inver. Mod. Initial' that stands for the inverse model solution using the initial mass transport, i.e., using no information from the Argo velocities. This solution uses the same *a priori* variance for each constraint than 'Inver. Mod. Veloc.' but a larger preliminary variance velocity assigned to the station pairs over the open ocean that is (3 cm/s)^2. The mass transport for both solutions is not significantly different but the uncertainty decreases using the Argo velocities. In the following, we will speak about the 'Inver. Mod Veloc.' solution.

Because the Mediterranean Sea exchanges water with the North Atlantic Ocean between our two bounding sections, we have also made an inverse model allowing for both an outflow of 1 Sv into the Mediterranean as described in Candela (2001) and an entrainment of a similar volume drawn from layers 4:5 into the Mediterranean Water (MW) as shown by Baringer and Price (1997), which then augments the transport of layers 6:7. This MW transformation process is usually ignored in basin scale inverses of the ocean circulation (Ganachaud, 2003), but we include it because it also gives some insight into the limitations of our method, and we believe it reflects a reality that can be used as one of the constraints of the problem. One can see (Fig. 4) for both of these solutions that the 36/24N sections present a predominant northward/southward flow in the upper 4 layers, while deeper layers have a net mass transport to the south. The MOC, as indicated by the the zonally-integrated northward flow in the upper 4 layers, is somewhat stronger at 24N with the MW constraint (Table 1), with some of that increase vanishing at 36N and contributing to the entrainment of Atlantic Water into the Mediterranean. We will now compare these estimates with previous ones made from individual hydrographic sections at both latitudes. In this, we will use only our transports from the thermocline layers (layers 1:4).

The 24 and 36N transatlantic sections have been occupied two times at the same time, 1957 (Fuglister, 1960) and 1981 (Roemmich and Wunsch, 1985). The 24N was again occupied in 1992 during the WOCE era (Parrilla et al., 1994), 1998 (Baringer and Molinari, 1999), and finally in 2004 (Bryden *et al.*, 2005b). As seen in Fig. 1c, the 1957 and 1992 sections were along 24N from the African shelf to the Bahama Bank, and the 1981, 1998 and 2004 sections were oriented to the northeast when approaching the African continent. Different authors have computed either accumulated volume transport or accumulated mass transport from the easternmost point to the west (Bryden *et al.*, 2005b; Ganachaud, 1999; Roemmich and Wunsch, 1985). In order to compare our estimates with previous, we have digitalized their original figures into accumulated transport (e.g. transport streamfunction) as a function of longitude. We use published inverse analyses of the historical data when they are available as our points for comparison. Because the results of Bryden *et al.* (2005b) are integrated in the top 1000 m, while we use density levels, we have had to apply a scale factor of 0.83 derived from our own results by the ratio of the transport of layers 1 to 4 vs. that of upper 1000 m.

The comparison of results (Fig. 5) for 36N shows a smaller eddy variability in accumulated mass transport than that from (Roemmich and Wunsch, 1985). As already seen, the reduced eddy variability is most likely a result of our use of 5 years of Argo float data, thereby reducing effects of individual eddies, which remain present in single hydrographic sections. Our section transport totals in all of the above comparisons show a difference from estimates from previous years for both solutions, i.e., for the case for no MW and MW transformation. This difference is not significant if we assume that the uncertainty of the integrated mass transport in 1957 and 1981, not shown in their manuscript, is similar to ours.

For 24N, we show a comparison of our accumulated mass transport and those as solutions of inverse models (Fig. 5b) and also those from a recent work carried out by Bryden *et al.* (2005b) that corresponds in time closest to our result (Fig. 5c), which indicates a strengthened upper layer interior flow to the south at 24N. Our estimates at 24N are not significantly different than earlier estimates from inverse models. We are led to the conclusion that there is no significant change in the upper limb of the MOC in the period 2003-2007, and that changes we see are not significantly different than previous findings going back to the IGY in 1957. The recent transport from 2004 section and sections carried out in 1981 and 1998 as computed from Bryden *et al.* (2005b) are within our error bars as well for the case of MW transformation. The MW solution shows a marginally significant reduction in the southward transport: the MW transformation thus affects the estimated overturning circulation at 24N. Most of the difference in the two inverse solutions is taken up at 24N from the eastern boundary.

The difference of using a single hydrographic section or a synoptic section is clearly seen in the Antilles Current, west of 70W at 24N. Antilles Current shows a large variability with transports above 1000 m varying between -15 and +25Sv (Johns *et al.*, 2008). A single hydrographic section could measure any transport in this range as is shown in Figure 5b. Bryden *et al.* (2005a) with a series of seven moorings over 11 years and Johns *et al.* (2008) with an array of six moorings over ~1 year obtained a transport for the Antilles Current of

5.1 and 6.0 Sv, respectively. From our data, mass transport west of 70W and shallower than 27.38 γn is 5.6±1.7 Sv, which is consistent with these previously published results.

Although we cannot make a top to bottom budget, our combined box model results indicate that the MOC is not decreasing with time at 24N, at least to the error (±3 Sv) which we ascribe to the thermocline waters. If we balance all the net northward flow in the upper 4 layers with southward flow in the lower limb of the MOC, we would estimate that ca. 12.8±3.0 Sv are involved in the zonally-averaged overturning circulation at 24N in the North Atlantic Ocean, and that this number has not changed significantly since 1957.

These calculations represent some new application of Argo data to ocean circulation studies. We have found that mean hydrography and reference level flow information from Argo are valuable additions to our ocean observing system, that one still needs other information (i.e. boundary current velocities or transports) to characterize the net upper level flow, and mass conservation 'constraints', before one can make statements about the flow below the level of Argo.

Appendix

A sensitivity test of the solution has been carried out by changing the variance assigned to the layer mass noise and the reference level velocity. The sensitivity test has consisted in considering an increase and a decrease in a 50% of each variance keeping the variance assigned to the Gulf Stream unchanged. For our solution the net imbalance is -1.8±1.9 Sv. For the rest of the solutions the imbalance is greater than its uncertainty except when the a priori variance of the reference level velocities is increased. In this case, the net imbalance is -1.4±2.1 Sv but the northward transport in the thermocline layer in 36N is only 5.0±3.9 Sv, leading us to disregard this solution.

Acknowledgments

The data used here were collected and made freely available by the International Argo Project and the national programs that contribute to it. (http://www.argo.net). Argo is a pilot program of the Global Ocean Observing System. This study used the data of YoMaHa'05 (Yoshinary *et al*., 2006) dataset of velocities derived from Argo float trajectories provided by APDRC/IPRC. This study has been partly funded by the MOC project (CTM2008-06438) funded by the Spanish Government and Feder. One of us (TJ) would like to acknowledge support from NSF Grant OCE-0241354 and NOAA/CICOR grant NA17RJ1223.

References

ArgoScienceTeam, 1998. On the design and implementation of Argo: An initial plan for a global array of profiling floats. International CLIVAR Project Office Report 21, GODAE Report 5, p. 32.

Baringer, M.O., Larsen, J.C., 2001. Sixteen years of Florida Current transport at 27ºN. Geophysical Research Letters 28 (16), 3179-3182.

Baringer, M.O., Molinari, R., 1999. Atlantic Ocean baroclinic heat flux at 24 to 26ºN. Geophysical Research Letters 26 (3), 353-356.

Baringer, M.O., Price, J.F., 1997. Mixing and spreading of the Mediterranean outflow. Journal of Physical Oceanography 27 (8), 1654-1677.

Bryden, H.L., Imawaki, S., 2001. Ocean Heat Transport. In: Siedler, G., Church, J., Gould, J. (Eds.), Ocean Circulation and Climate. Academic Press, pp. 455-474.

Bryden, H.L., Johns, W.E., Saunders, P.M., 2005a. Deep western boundary current east of Abaco: Mean structure and transport. Journal of Marine Research 63 (1), 35-57.

Bryden, H.L., Longworth, H.R., Cunningham, S.A., 2005b. Slowing of the Atlantic meridional overturning circulation at 25ºN. Nature 438 (7068), 655-657.

Candela, J., 2001. Mediterranean Water and Global Circulation. In: Siedler, G., Church, J., Gould, J. (Eds.), Ocean Circulation and Climate. Academic Press, pp. 419-429.

Cunningham, S.A., Kanzow, T., Rayner, D., Baringer, M.O., Johns, W.E., Marotzke, J., Longworth, H.R., Grant, E.M., Hirschi, J.J.M., Beal, L.M., Meinen, C.S., Bryden, H.L., 2007. Temporal variability of the Atlantic meridional overturning circulation at 26.5ºN. Science 317 (5840), 935-938.

Fraile-Nuez, E., Hernandez-Guerra, A., 2006. Wind-driven circulation for the eastern North Atlantic Subtropical Gyre from Argo data. Geophysical Research Letters 33 (3), L03601, doi:10.1029/2005GL025122.

Fuglister, F., 1960. Atlantic Ocean atlas of temperature and salinity profilers and data from the International Geophysical Year of 1957-1958. Woods Hole Oceanographic Institution Atlas Series, p. 209.

Ganachaud, A., 1999. Large scale oceanic circulation and fluxes of freshwater, heat, nutrients and oxygen, Joint Program in Physical Oceanography of Massachusetts Institute of Technology and Woods Hole Oceanographic Institution.

Ganachaud, A., 2003. Large-scale mass transports, water mass formation, and diffusivities estimated from World Ocean Circulation Experiment (WOCE) hydrographic data. Journal of Geophysical Research-Oceans 108 (C7), 3213, doi:10.1029/2002JC001565.

Hadfield, R.E., Wells, N.C., Josey, S.A., Hirschi, J.J.-M., 2007. On the accuracy of North Atlantic temperature and heat storage fields from Argo. Journal of Geophysical Research-Oceans 112, C01009, doi:10.1029/2006JC003825.

Halkin, D., Rossby, T., 1985. The structure ans transport of the Gulf-Stream at 73ºW. Journal of Physical Oceanography 15 (11), 1439-1452.

Hogg, N.G., 1992. On the transport of the Gulf-Stream between Cape-Hatteras and the Grand-Banks. Deep-Sea Research Part a-Oceanographic Research Papers 39 (7-8A), 1231-1246.

IPCC, 2001. Climate Change 2001: The scientific basis. Contribution of working group I to the third assessment report of the Intergovernmental Panel on Climate Change, p. 881.

Jackett, D.R., McDougall, T.J., 1997. A neutral density variable for the world's oceans. Journal of Physical Oceanography 27 (2), 237-263.

Johns, W.E., Beal, L.M., Baringer, M.O., Molina, J.R., Cunningham, S.A., Kanzow, T., Rayner, D., 2008. Variability of shallow and deep western boundary currents off the Bahamas during 2004-05: Results from the 26N RAPID-MOC array. Journal of Physical Oceanography 38 (3), 605-623.

Levitus, S., Boyer, T., 1994. World Ocean Atlas 1994. 4, Temperature. p. 129.

Levitus, S., Burgett, R., Boyer, T., 1994. World Ocean Atlas 1994. 3, Salinity. p. 111.

Parrilla, G., Lavin, A., Bryden, H., Garcia, M., Millard, R., 1994. Rising temperatures in the Subtropical North-Atlantic ocean over the past 35 years. Nature 369 (6475), 48-51.

Pedder, M.A., 1993. Interpolation and filtering of spatial observations using successive corrections and Gaussian filters. Monthly Weather Review 121 (10), 2889-2902.

Roemmich, D., Wunsch, C., 1985. Two transatlantic sections - meridional circulation and heat-flux in the Sub-Tropical North-Atlantic ocean. Deep-Sea Research Part a-Oceanographic Research Papers 32 (6), 619-664.

Wong, A.P.S., Johnson, G.C., Owens, W.B., 2003. Delayed-mode calibration of autonomous CTD profiling float salinity data by theta-S climatology. Journal of Atmospheric and Oceanic Technology 20 (2), 308-318.

Wunsch, C., 1996. The Ocean Circulation Inverse Problem. Cambridge University Press.

Wunsch, C., Heimbach, P., 2006. Estimated decadal changes in the North Atlantic Meridional Overturning Circulation and heat flux 1993-2004. Journal of Physical Oceanography 36 (11), 2012-2024.

Yoshinari, H., Maximenko, N.A., Hacker, P.W., 2006. YoMaHa'05: Velocity data assessed from trajectories of Argo floats at parking level and at the sea surface. IPRC Technical Note No.4, p. 16.

Figure Captions

Figure 1. a) Locations of every temperature and salinity vertical profile in the period 2003-2007 from Argo data used to objectively interpolate the temperature and salinity every degree in longitude at 24 and 36N; b) repeated hydrographic sections taken across 24 and 36N in the International Geophysical Year (IGY, 1957), 1981, the World Ocean Circulation Experiment (WOCE, 1992), 1998 and 2004. The synthetic sections used in this work are also shown; c) parking depth velocity locations at 1000/1500 m (red/blue) from (Yoshinari *et al.*, 2006) used to objectively estimate the velocity at 1000/1500 m west/east of 45W at the mean position used for temperature and salinity.

Figure 2. Vertical sections of a), c) potential temperature (^{o}C) and b), d) salinity for the 36N, 24N sections, respectively, from the objective analysis using 3,349 profiles of Argo data in the period 2003-2007. Gamma_n (γ_n) isolines are shown in each plot.

Figure 3. Mean velocities from the objectively interpolated Argo floats at reference levels (blue) and adjusted velocities from the solution of the inverse model (red) and for the MW solution (red dashed) for a) 36N, and b) 24N.

Figure 4. a) Initial integrated mass transport as a function of density layer for the sections at 24N+Florida Strait (blue), and at 36N (red), together with their divergence (black line). The mass transport is computed using the adjusted velocities of Fig. 3 (blue line) and 22 cm/s for

the Florida Strait; b) as in a) but also using the velocities from the inverse model as seen in Fig. 3 (red line). For c) as in b) but using the inverse solution with MW constraints (Fig. 3, red dashed line). In each of these cases, positive/negative sign means north/south flow. The sign of the divergence transport is taken positive/negative for flow out of/into the box for all cases. We interpret the convergence in layer 1 and divergence in layer 2 as reflecting the transformation of surface waters into subtropical mode waters formed between the two latitudes.

Figure 5. Accumulated volume transport for layers 1:4, integrated from the eastern boundary to the west for a) 36N, b) 24N. IGY and 1981 are published in (Roemmich and Wunsch, 1985), WOCE transport is published in (Ganachaud, 1999) as mass transport. Original data are divided by the mean density of the ocean to convert them to volume transport; and c) same as b) but using transports published in (Bryden *et al.*, 2005b). In this case, we have applied a scale factor of 0.83 derived from our own results to obtain the transport in the upper 1000 m from transport in layers 1:4. Our inverse solution including the MW transformation is shown as the thick red dashed line.

Table 1

		Florida (Sv)	24ºN (Sv)	Florida+24º N (Sv)	36ºN (Sv)
Total γ_n=Surface:27.922	Initial	32.4	1.1	33.5	27.4
	Velocity Data	32.4	-8.4	24.0	11.5
	Inver. Mod. Initial	32.3±0.1	-26.5±5.6	5.8±5.6	4.1±5.7
	Inver. Mod. Veloc.	32.3±0.1	-26.9±4.6	5.4±4.6	3.6±4.7
	Inver. Mod. Med.	32.3±0.1	-23.0±4.6	9.3±4.6	8.0±4.7
Layers 1-4 γ_n=Surface:27.38	Initial	31.4	-1.8	29.6	18.7
	Velocity Data	31.4	-7.3	24.1	12.4
	Inver. Mod. Initial	31.3±0.1	-18.5±3.7	12.8±3.7	10.5±3.8
	Inv. Mod. Veloc.	31.3±0.1	-18.5±3.0	12.8±3.0	10.4±3.1
	Inver. Mod. Med.	31.3±0.1	-16.4±3.0	14.9±3.0	11.5±3.1
Layers 5-7 γ_n=27.38:27.922	Initial	1.0	2.9	3.9	8.7
	Velocity Data	1.0	-1.1	-0.1	-0.9
	Inver. Mod. Initial	1.0±0.0	-8.0±4.3	-7.0±4.3	-6.4±4.3
	Inver. Mod. Veloc.	1.0±0.0	-8.4±3.5	-7.4±3.5	-6.8±3.5
	Inver. Mod. Med.	1.0±0.1	-6.6±3.5	-5.6±3.5	-3.5±3.5

Initial stands for the geostrophic mass transport (reference layer γ_n=27.922 kg/m^3) and initial Ekman transport included in the first layer. The Florida mass transport has been obtained using a velocity of 22 cm/s in each station pair. *Velocity Data* stands for geostrophic mass transport using the reference velocity from Argo data and 22 cm/s in each station pair for the Florida mass transport. The initial Ekman transport is included in the first layer. *Inv. Mod. Initial* stands for geostrophic mass transport after the inverse model using the initial transports. *Inv. Mod. Veloc.* stands for geostrophic mass transport after the inverse model using the transports adjusted to the reference velocity from Argo data. *Inv. Mod. Med.* uses the data as previous inverse model considering Mediterranean Water transformation. Adjusted Ekman transport as obtained from the inverse model is included in the first layer. The initial Ekman transport as obtained by satellite data is -2.2 Sv at 36N and 5.3 Sv at 24N. The adjusted Ekman transport as obtained from the inverse model is −1.8±0.4 Sv at 36N and 3.1±1.0 Sv at 24N. All signs are geographic.

Figure 1

Click here to download Figure: Figure_1.eps

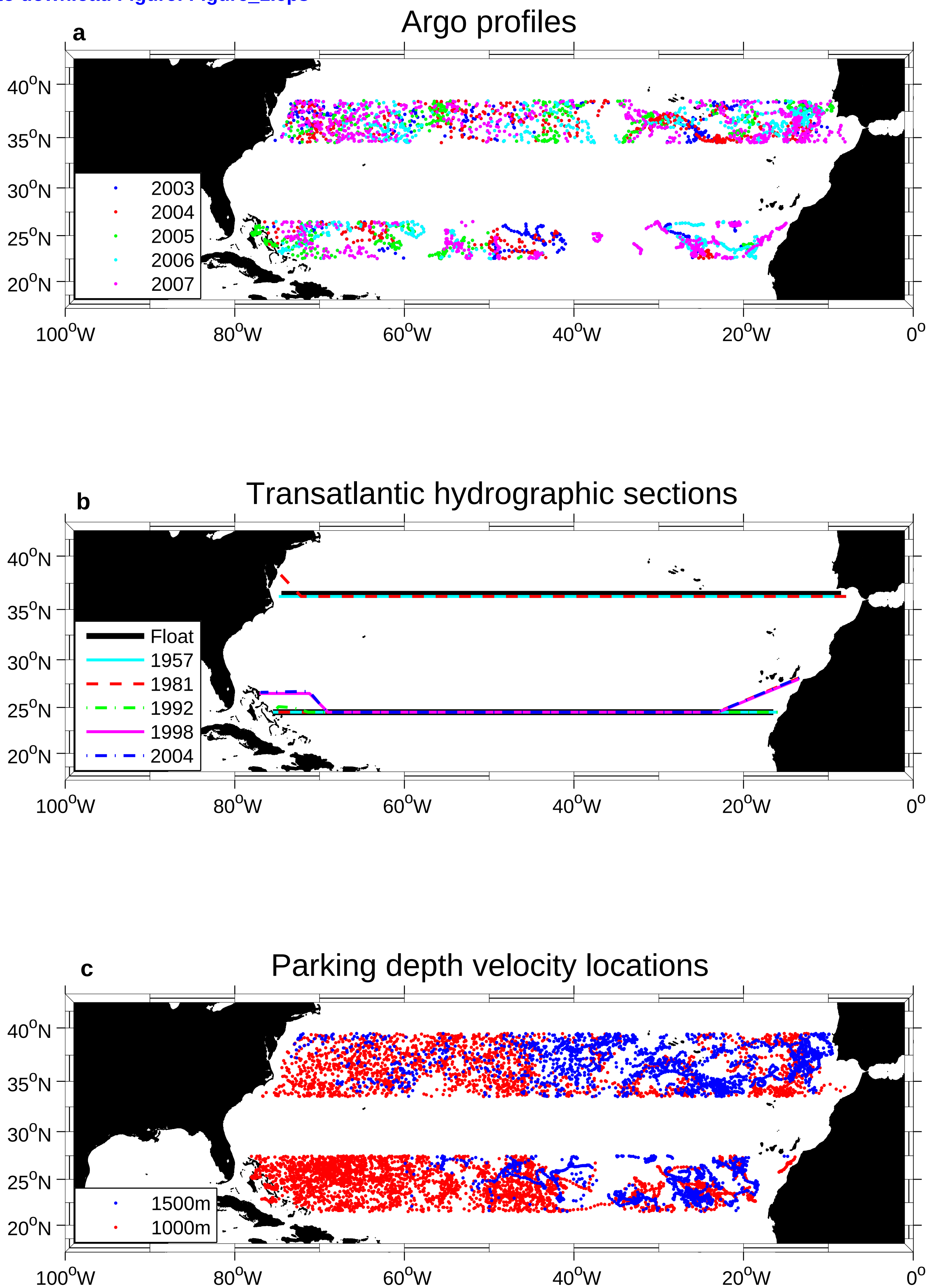

Figure 2

Click here to download Figure: Figure_2.eps

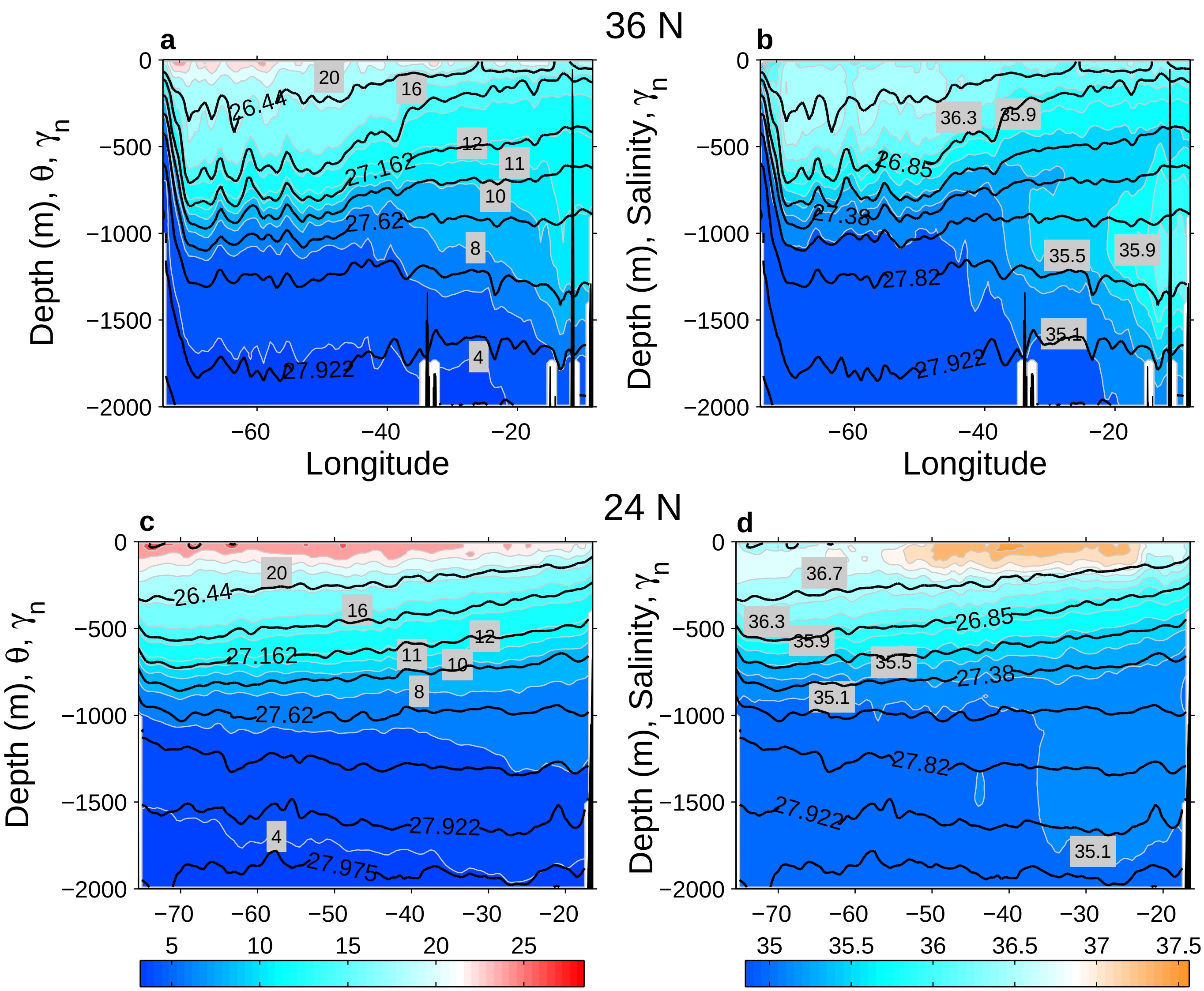

Figure 3

Click here to download Figure: Figure_3.eps

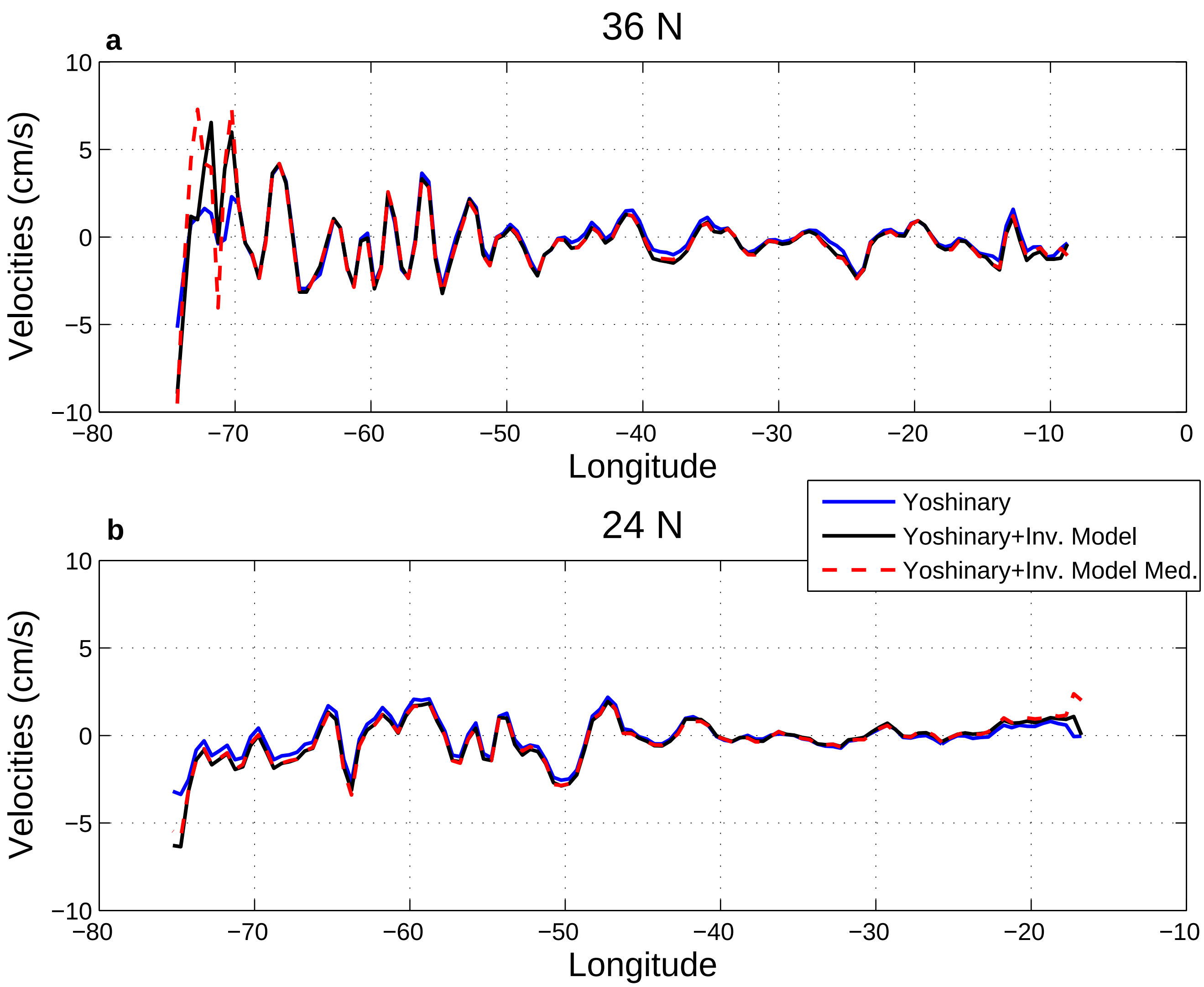

Figure 4
Click here to download Figure: figure_4.eps

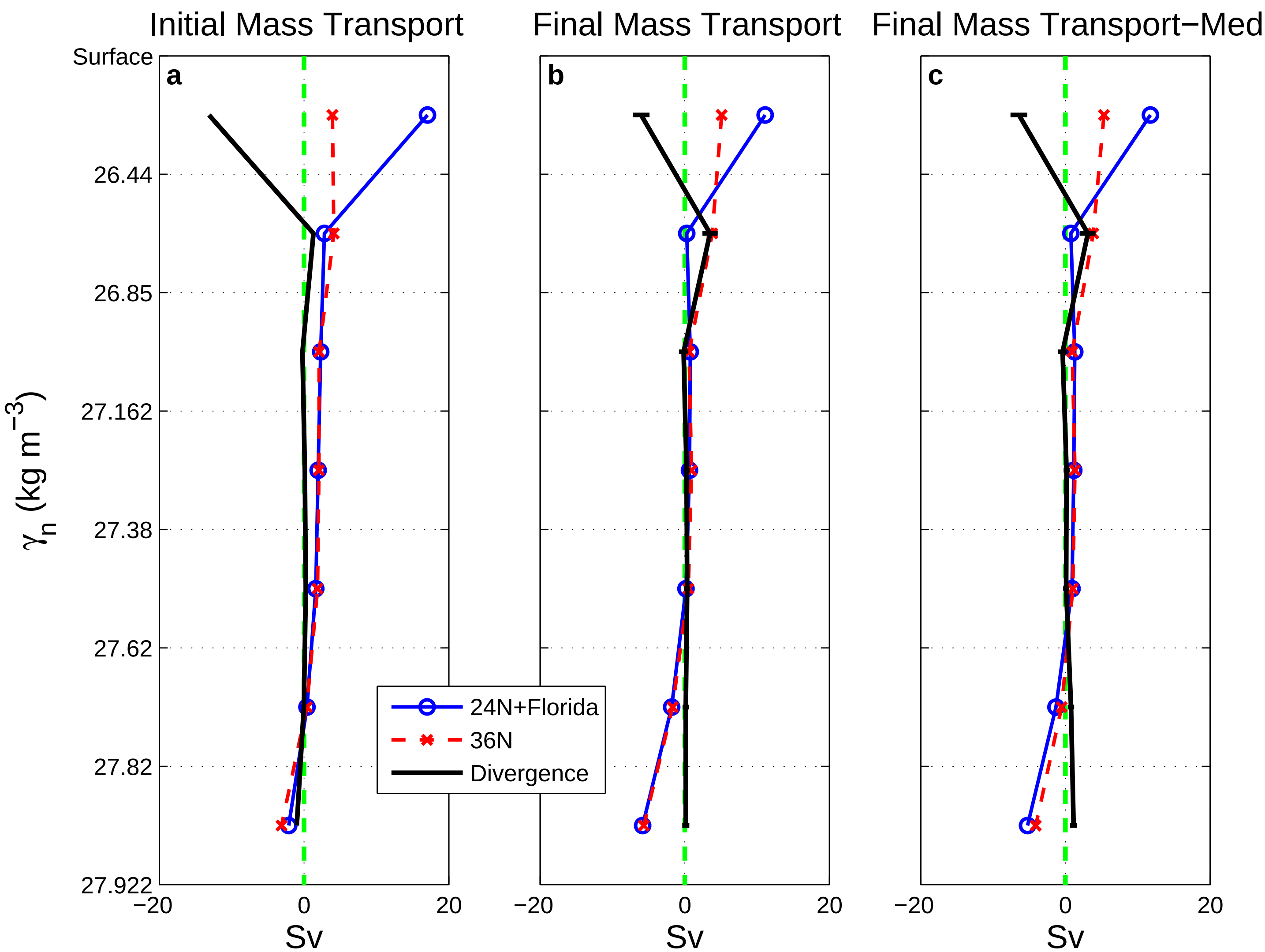

Figure 5

Click here to download Figure: Figure_5.eps